EPJ Web of Conferences **8**, 07005 (2010)
DOI: 10.1051/epjconf/20100807005
© Owned by the authors, published by EDP Sciences, 2010

^{7}Li neutron-induced elastic scattering cross section measurement using a slowing-down spectrometer

G. Kessedjian[a], O. Méplan, A. Billebaud, R. Brissot, S. Chabod, V. Ghetta, M. Heusch, and E. Liatard

LPSC, Université Joseph Fourier Grenoble 1, CNRS/IN2P3, Institut Polytechnique de Grenoble, 38000 Grenoble, France

Abstract. A new integral measurement of the ^{7}Li neutron induced elastic scattering cross section was determined in a wide neutron energy range. The measurement was performed on the LPSC-PEREN experimental facility using a heterogeneous graphite-LiF slowing-down time spectrometer coupled with an intense pulsed neutron generator (GENEPI-2). This method allows the measurement of the integral elastic scattering cross section in a slowing-down neutron spectrum. A Bayesian approach coupled to Monte Carlo calculations was applied to extract ^{natural}C, ^{19}F and ^{7}Li elastic scattering cross sections.

1 Motivation

In the past, Oack Ridge National Laboratory developed the molten salt reactor experiment MSRE [1] as a starting for molten salt reactor research plan [1]. Since few years the LPSC has improved this kind of system by developing the Molten Salt Fast Reactor (MSFR). In this concept, the fuel, in liquid phase, is also the neutron moderator and the coolant. This fuel is based on a liquid fluoride salt. It was demonstrated that the breeding potential of this concept depends strongly on the number of available neutrons in the core [2]. Consequently, to avoid neutron losses through ^{6}Li(n, t) capture reactions only ^{7}Li isotope has to be content in the salt. In the Thorium Molten Salt Fast Reactor concept (Th-MSFR), the fuel-coolant is defined as ^{7}LiF(0.775)-^{232}ThF$_4$(0.20)-^{233}UF$_4$(0.025) (mass proportion). A reaction cross section sensitivity analysis was performed which results are reported in the table 1 [3]. In regard to the sensitivity of K_{eff} multiplication factor, the most important reactions are captures on ^{232}Th and ^{233}U and fission of ^{233}U. In regard to the moderation, the light nuclei were considered to define correctly the neutron spectrum.

2 Slowing-down time spectrometer set-up

We performed a measurement of an integral ^{7}Li elastic scattering cross section in a slowing-down time neutron spectrum in a heterogeneous graphite slowing-down time spectrometer. Classical slowing-down spectrometers are generally built with lead blocks as heavy elements allows a better energy resolution than lighter elements. From 1 eV up to 10 keV neutron energy range, the neutron slowing-down time is mainly due to elastic scatterings. At higher energies, inelastic scattering process is needed to describe correctly the time-energy correlation [4]. With light elements like graphite and low energy neutrons, we have only access to the mean slowing down time which is a function of the elastic scattering cross section. However, for graphite, inelastic reactions appear starting from 4.7 MeV. As a consequence, this reaction does not perturb the energy-time correlation for thermal and epithermal neutron

[a] e-mail: kessedjian@lpsc.in2p3.fr

This is an Open Access article distributed under the terms of the Creative Commons Attribution-Noncommercial License 3.0, which permits unrestricted use, distribution, and reproduction in any noncommercial medium, provided the original work is properly cited.

Article available at http://www.epj-conferences.org or http://dx.doi.org/10.1051/epjconf/20100807005

Table 1. Sensitivity coefficients of Th-MSFR for 33-group ENDF/B-V calculation in regard to principal reaction cross sections.

Cross section	capture	fission	Elastic	inelastic	nu
^{233}U	−0.054	0.542	0.001	−0.0001	0.984
^{232}Th	−0.475	0.009	0.014	−0.0027	0.015
^{19}F	−0.015	–	0.087	−0.0049	–
^{7}Li	−0.0003	–	0.023	−0.0003	–

energies. Thus, graphite spectrometer allows the validation of the elastic scattering cross sections of light nuclei. Previous experiments have shown the feasibility of the experiment [5–7].

2.1 Presentation of PEREN facility

The graphite slowing down time spectrometer used in the PEREN facility is consists in a graphite cylinder of 1 m in diameter and height. Using the D(d, n)t reactions, a pulsed deuteron source of 220 keV provides intense neutron pulses of $E_n \sim 3$ MeV (GENEPI [12]). The titanium-deuterium target (TID) is placed in the middle of the graphite matrix. In the core of this spectrometer, we positioned a gamma detector (with a YAP scintillator) coupled to a resonant capture target, here in gold. The γ flash due to the interaction of deuteron pulse with the target backing (made of copper) gives the start for the acquisition and the gamma rays emitted by the ^{197}Au(n, γ) capture provides the slowing-down time (Fig. 1). Three configurations of the spectrometer were combined to extract the ^{7}Li elastic scattering cross section. The first configuration is a heterogeneous LiF-Graphite spectrometer. The mean value of the slowing down time corresponds to a combination of cross sections and densities of the all elements present in the spectrometer. A second configuration describes as a heterogeneous Teflon-graphite spectrometer used to obtain the fluorine contribution in the slowing-down time spectrum. The last configuration is a pure graphite spectrometer to cross-check and validate the experimental set-up.

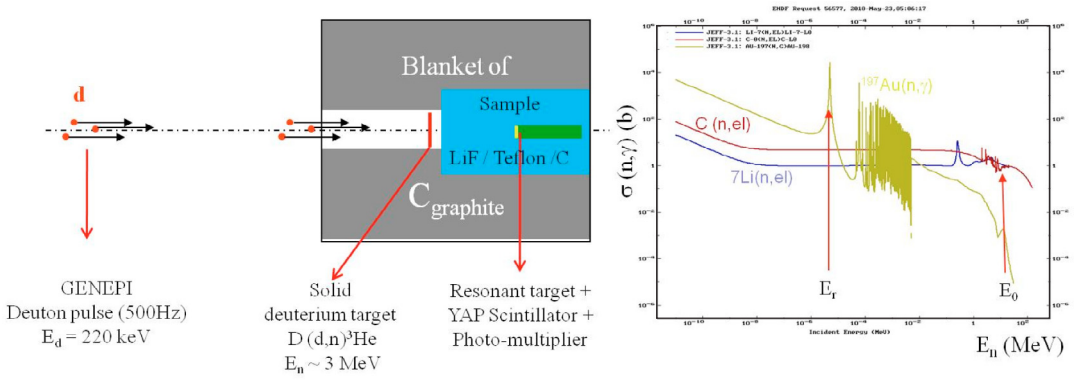

Fig. 1. PEREN Facility – Heterogeneous Sample-Graphite spectrometer. On right, the comparison of graphite and ^{7}Li elastic scattering cross sections and gold cross section.

^{7}LiF ingots are synthesized in gloves boxes using a ^{7}LiF powder obtained by fluorination of ^{7}Li hydroxide provided by Cogema. Several preliminary fusions of the powder were performed to elaborate the blocks used for the final ingots melting. Solidification took place in a graphite crucible, in a three areas furnace with very slow temperature slope rate. Hollow ingot is molded in two pieces owing in order to minimize internal strain.

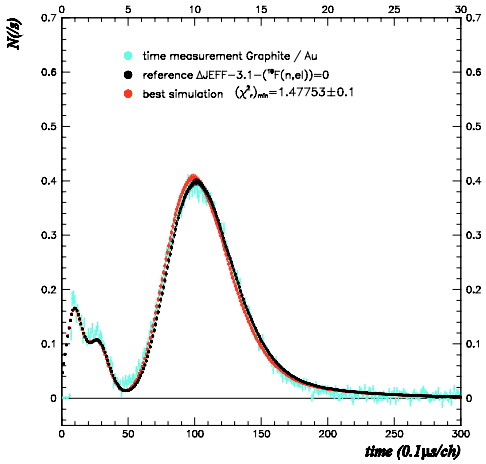

Fig. 2. Experimental (blue) and simulated (red) slowing down time spectra: resonant capture yields N(t) as a function of time in channel (0.1 μs/ch).

2.2 Experimental data analysis

The characteristic of a slowing down time spectrometer is the energy-time correlation described by the following relation [7]:

$$E_T = \frac{E_0 T_0}{(T_r + T_0)^2} \tag{1}$$

where E_0 is the energy of source neutrons, T_0 the characteristic slowing down time function of the properties of the materials present in the spectrometer (cross sections and densities) and Tr the mean resonant time. In Fig. 2 a slowing down time spectrum is presented after subtraction of the background induced by the components of the YAP scintillator and photomultiplier. For each capture resonance of the gold target, we observe a peak in a time spectrum which position and shape are function of the integral (n,el) cross section from the source neutron energy, E_0, down to the resonant energy E_r. Monte Carlo calculations were performed using MCNP5.1 and MURE codes [8] to extract the ^{7}Li(n,el) cross section from the recorded time spectrum . We have taken into account the compositions of graphite, lithium fluoride and Teflon blocks, the geometry of the gold target and detector as well as the PEREN facility configuration and environment.

3 Neutron induced elastic scattering cross section analysis

3.1 Bayesian approach

In this experiment, we measured the resonant time spectrum, T_r, as a function of the elastic scattering cross sections and densities (ρ) of the spectrometer components:

$$T_r = N_r(t) = f(^{nat}C(n,el); ^{19}F(n,el); ^{7}Li(n,el); \rho_c; \rho_{LiF}) \tag{2}$$

and we want to infer the ^{7}Li elastic scattering cross section as a function of data:

$$^{7}Li(n,el) = g(T_r; ^{nat}C(n,el); ^{19}F(n,el); ^{7}Li(n,el); \rho_c; \rho_{LiF}) \tag{3}$$

To solve the equation (3), we have based our analysis on a Bayesian approach [9, 10]:

$$P(H_i|data;\eta) = \frac{P(data|H_i;\eta)\cdot P(H_i)}{P(data)} \tag{4}$$

$$\text{If } \varepsilon_{data} \subset \varepsilon_H, \text{ then } P(data) = \sum_i P(data|H_i;\eta)\cdot P(H_i) \tag{5}$$

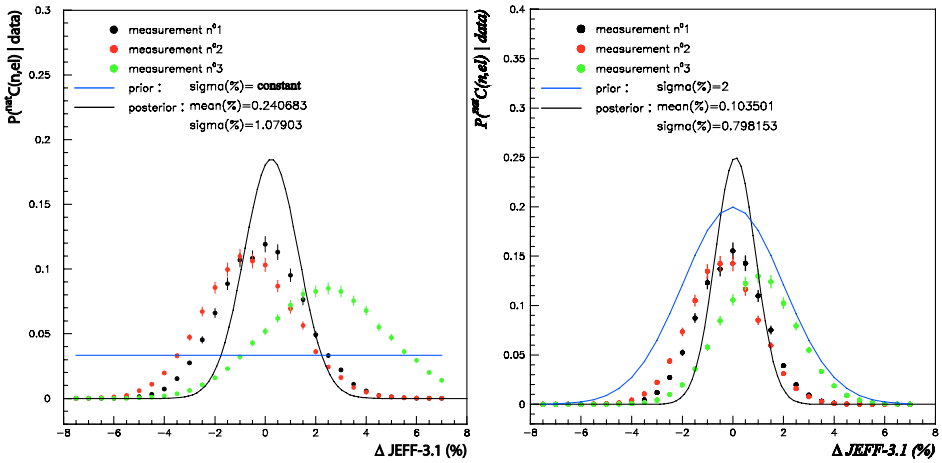

Fig. 3. Left: probability density function (PDF) as a function of JEFF3.1 deviation of graphite evaluation for a constant prior. The black line describes the final posterior of our measurement (without error on graphite density). Right: PDF of C(n,el) cross section compared to the JEFF3.1 evaluation for a Gaussian prior centred to JEFF3.1 and a 2% standard deviation.

where the "data" are the resonant time spectrum (T_r), "H_i" the assumption on ^{7}Li(n, el) cross section plateau and η the nuisance parameters as graphite and fluorine cross sections and densities of the components. The probability of hypothesis "H_i" given data and nuisances "η" is called the posterior probability. $P(H_i)$ represents the knowledge on the parameter sought and is called prior. The probability of data given hypothesis and nuisances, $P(data|H_i,\ \eta)$, is proportional to the likelihood function. The normalisation by the probability of data, $P(data)$, erases the proportionality between the likelihood function and the probability $P(data|H_i,\ \eta)$. For a Gaussian propagation of uncertainties, the likelihood function L is defined as [9]:

$$P(data|H_i;\eta) \propto L(data|H_i;\eta) \propto \exp\left(-\frac{\chi^2}{2}\right) \tag{6}$$

with χ^2 being the least square function.

3.2 Homogeneous graphite spectrometer

Using a pure graphite spectrometer, we have measured three sets of data with a gold resonant target. First, we present the probability density function (PDF) of C(n,el) cross section in comparison to the JEFF3.1 evaluation in Fig. 3. We note a perfect agreement between these three measurements. Each point is the result of a MCNP calculation performed with different values of JEFF3.1 C(n,el) cross section plateau. The standard deviation of each measurement is around 1.7% and the final posterior of all data are defined by a mean value of 0.2% (compared to JEFF3.1) and a standard deviation of 1.2% taking into account a 0.5% standard deviation on the graphite density. This analysis with a constant prior gives the spectrometer resolution in regard to C(n,el) cross section: R(C(n,el))~1.7%.

In a second time, the precision on the available experimental data in the C(n,el) cross section plateau is around 2%. This resolution defines the prior knowledge on this cross section. Thus, a second calculation with a new prior led to the final measurement on graphite. The posterior density probability function is closed to JEFF3.1 assessment with a 0.1% mean value (in comparison to JEFF3.1 C(n,el) evaluation) and a 1%standard deviation considering the 0.5% standard deviation of graphite density. According to the time-energy correlation, the weight W(E_n) of neutron induced elastic scattering cross section at neutron energy E_n, can be defined as the ratio of the differential "life time" of neutron at E_n to the total slowing-down time. This weight represents the importance of the cross section value at

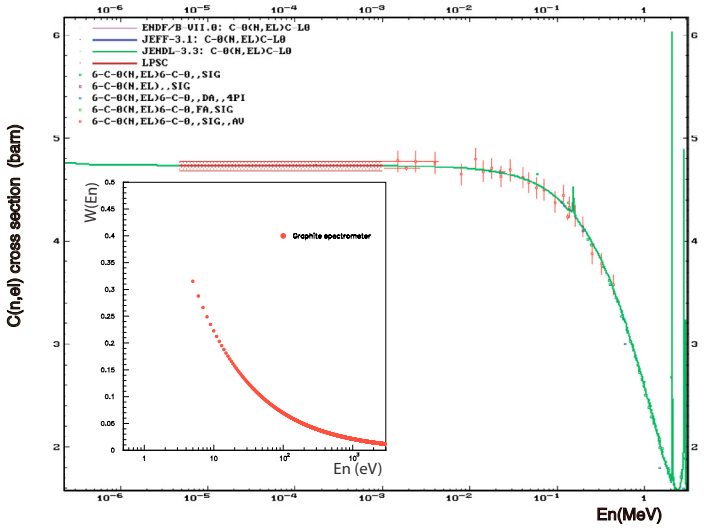

Fig. 4. Integral elastic scattering cross section plateau from the gold resonant energy 4.9 eV up to 1 keV [11]. Insert: the weight of the differential graphite elastic scattering cross section on the integral cross section measurement as a function of the neutron energy E_n.

neutron energy E_n in the integral cross section measurement for a gold resonant target ($E_r = 4.9$ eV) and a source neutron at $E_0 = 3$ MeV (fig. 4).

3.3 Heterogeneous graphite-Teflon and graphite-lithium fluoride spectrometers

Similar studies were performed for two heterogeneous spectrometer configurations. The first configuration considered here is the graphite-Teflon spectrometer with a gold resonant target. In this configuration, the resonant time, Tr, depends on both graphite and fluorine elastic scattering cross sections as well as densities (ρ) of graphite and Teflon blocks. To determine the probability density function of ^{19}F(n,el) cross section, we have included in the calculations the resolution of the spectrometer in regards of C(n,el) cross section:

$$P(^{19}F(n,el)|T_r;\eta) = \frac{P(T_r|^{19}F(n,el);\eta)\cdot P(^{19}F(n,el))}{P(T_r)} \tag{7}$$

data are the resonant time spectrum with Teflon $T_r = N_r(t)$ and η characterises the nuisance parameters: $\eta = C(n,el)$; ρ_c; ρ_{Teflon}. The resolution on C(n,el) cross section gives a limit on the precision on the mean resonant time value for the Teflon block. To take into account this uncertainty on the comparison between experimental spectrum and Monte-Carlo calculated spectra, we consider the least square given by:

$$\chi^2(^{19}F(n,el);T_r;R(C(n,el)) = \sum_i \frac{(N^{cal}(ti) - N^{\exp}(ti))^2}{\sigma^2(N^{cal}) + \sigma^2(N^{\exp}) + \left(\frac{\partial N^{\exp}(t_i)}{\partial t_i}\right)^2 \cdot \sigma^2{}_{\langle Tr\rangle}} \tag{8}$$

where statistical uncertainties of experiments ($N^{\exp}$) and Monte Carlo calculations (N^{cal}) are added to the uncertainty on the mean resonant time given by:

$$\frac{\sigma_{\langle Tr\rangle}}{\langle T_r\rangle} = S_{\langle Tr\rangle;C(n,el)}\cdot R(C(n,el)) \tag{9}$$

S⟨Tr⟩; C(n,el) and R(C(n,el) are, respectively, the sensitivity of mean resonant time to the C(n, el) cross section and the resolution of the slowing down time spectrometer in regard to the C(n,el)

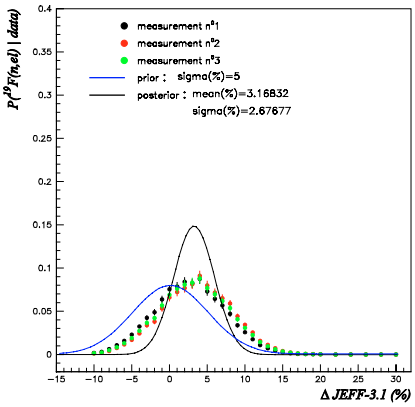

Fig. 5. Experimental probability density function of ^{19}F(n, el) cross section measurements as a function of deviation from the JEFF3.1 assessment (preliminary results).

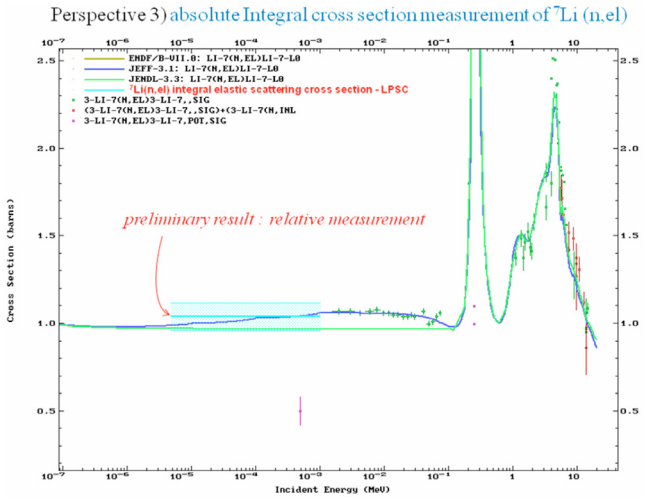

Fig. 6. Experimental probability density function of ^{19}F(n, el) cross section compared to JEFF3.1 assessment (preliminary results).

cross section. The probability density function of ^{19}F(n,el) cross section compared of JEFF3.1 (Fig. 5) were calculated with a 5% standard deviation on the prior probability, corresponding to the present knowledge of ^{19}F(n, el) cross section plateau. The preliminary result matches rather well the JEFF3.1 assessment with a mean deviation of 3.1 (±2.7)% compared to JEFF3.1. We can extract from this analysis the correlation between ^{19}F(n, el) and C(n,el) cross section measurements that is found equal to −0.25.

For the heterogeneous Lithium fluoride – Graphite spectrometer configuration, the ^{19}F(n, el) and C(n, el) cross sections and the densities of components define the nuisance parameters η. Many cracks in the LiF block prevent from an exact determination of the lithium density. Presently, we have only determined the ratio of ^{7}Li(n, el) and ^{19}F(n, el) cross sections. For the JEFF3.1 assessment of ^{19}F(n, el) cross section, we obtain an elastic scattering cross section plateau at 1.04 ± 0.8 barn with a 5% standard deviation from the JEFF3.1 ^{19}F(n, el) evaluation (Fig. 6). The result is in better agreement with JEFF3.1 and ENDF-BVII evaluations than with the JENDL library. However the resolution of our experiment cannot exclude the JENDL library values. Moreover, an integral measurement does not provide access to the structures of the ^{7}Li elastic scattering plateau as defined by JEFF3.1 and ENDF-BVII libraries.

4 Conclusion and perspectives

First experimental results obtained with heterogeneous graphite slowing down time spectrometers were presented: they provide integral elastic scattering cross section measurements in the 1–1000 eV neutron energy range. Using a Bayesian analysis, three complementary experiments have allowed the determination of the probability density functions of graphite and fluorine elastic scattering cross sections. The ratio of ^{7}Li to ^{19}F elastic scattering cross sections was deduced from the experiments. We have obtained a new ^{7}Li integral cross section at low neutron energy range in agreement with the JEFF3.1and ENDF-BVII libraries.

This work was supported by the CNRS PACEN and GEDEPEON programs. The authors thank the GENEPI accelerator staff of the LPSC and J. Bouvier for their great support during the experiments and D. Heuer, E. Merle-Lucotte, X. Doligez, A. Bidaud, M. Hoogmoed, H.E. Thyèbault, A. Nuttin for the discussions on reactor physics.

References

1. P. Haubenreich, J.R. Engel, Nuclear application & technology, Vol. **8**, pp 118–136, feb. 1970
2. Nuttin, A., *PhD thesis*, Université Joseph Fourier - Grenoble I. (2002)
3. M. Hoogmoed, A. Bidaud, X. Doligez, *International Conference on Nuclear Data for Science and Technology 2010*, Jeju Island, Korea, (2010)
4. T.D. Beynon, J. Phys. D: Appl. Phys., Vol. **5** (1972)
5. A. Takahashi et al., Journal of Nuclear Science and Technology, 4[10] , p. 503~511 (October 1967)
6. A.I.Hawari, Nuclear Instruments and Methods in Physics Research A **422** (1999) 846–851
7. N. Thiollière, *PhD thesis*, Université de Grenoble (2002)
8. Méplan, O. et al., *MURE, MCNP Utility for Reactor Evolution: couples Monte-Carlo transport with fuel burnup calculations*. <http://www.nea.fr/abs/html/nea-1845.html>. Data Bank Computer Program Services, OECD Nuclear Energy Agency (2009)
9. A. Putze, *PhD thesis*, Université Joseph Fourier - Grenoble I (2009)
10. J. Limmemann, et al., Calculation Confidence Limits, article in preparation
11. National nuclear Data Center, Brookhaven National Laboratory, http://www.nndc.bnl.gov/
12. L. Perrot et al., Nuclear Science and Engineering **144** (2003) 142–156